Ezratty Supplementary Figure Legends

Figure S1, related to Fig1. Ciliagenesis during embryonic epidermal stratification. (A) Confocal immunofluorescence (IF) of whole-mount epidermis (planar views) was imaged for embryonic days and antibodies (Abs) indicated (color-coding according to secondary Abs) in basal and suprabasal epidermal cells. Arrows denote individual primary cilia, visualized by anti-acetylated tubulin; nuclei marked by DAPI**. (B)** Ciliogenesis in E15.5 epidermis from α-catenin and $\beta 1$ integrin cKO and WT mice. Arrows denote individual apically oriented cilia numerous in WT but not mutant epidermis. Scale bars= 10μM.

Figure S2, related to Fig2. Depletion of kinesin II *in vitro*: inhibition of ciliogenesis but variability in non-ciliary effects. (A-B) Immunofluorescence of LV-Cre-transduced *Kif3a* (fl/+) (WT) or (fl/fl) (KO) mouse keratinocytes (MKs) with Abs indicated. Arrowheads in (A) denote cilia, present only in kinesin II(+) MKs. Note alterations at cell-cell borders, typically reinforced by cortical MTs (MTs), also defective in *Kif3a*-null MKs (*high magnification of boxed regions in A and arrowheads in B). Bar, 10μM**. (C)** Quantification of ciliogenesis in WT vs Kif3a ckO MKs. Histograms are mean data averaged from 2 independent experiments**. (D)** Representative immunoblots of lysates from MKs expressing *Ift*-shRNAs indicated (S, scrambled shRNA). HPRT, loading control. **MT dynamics in MKs depleted of Ift74.** P0 MKs were infected with lentiviruses expressing either scrambled or *Ift74-1* shRNA and harboring a puromycin resistance gene. Puromycin-selected cell lines were then prepared and confirmed to express the appropriate shRNA. These lines either expressed IFT74 at normal levels or at levels ~10% of WT (see main text). **(E)** Table summarizing MT dynamics parameters. Individual MTs were imaged in MK cell lines stably expressing scrambled or *Ift74* shRNA and transiently transfected with mCherry-tubulin to visualize MTs. Images were acquired every 10 seconds for 5-15 minutes and analyzed to determine parameters of MT dynamics. Table1 summarizes the % of time that individual MTs spent pausing, growing, or depolymerizing. Note that MTs from scrambled control and *Ift74* depleted cells showed equivalent MT dynamics in this analysis**. (F**) Individual frames from time lapse microscopy showing examples of MT dynamics in scrambled control or *Ift74-1* depleted keratinocytes. * denotes examples of individual MTs that either persist or grow as indicated in each frame. Time is min:sec. Bar, 2μM.

Figure S3, related to Fig4. *Kif3a* mutant epidermis does not show evidence of enhanced apoptosis

(A) *Kif3a* cKO tissue did not show elevated levels of activated caspase 3, a marker of apoptosis. We occasionally detected activated caspase 3 positive cells in the dermis (arrow in WT image). *Kif3a* cKOs were generated on a YFP Rosa 26 loxstoplox background, where cKO cells that express active Cre recombinase are YFP(+) (shown). Bar, 30μM.

Figure S4, related to Fig5. (A) Diagram of Notch reporter construct used in both *in vitro* and *in vivo* studies. **(B**) Treatment of MKs with choral hydrate removes primary cilia but does not affect levels of acetylated tubulin or overall MT organization, as visualized with anti-α-tubulin. MKs were grown to confluence and then shifted to 2mM Ca^{+2}media containing 2mM chloral hydrate for 48 hrs. Scale bar=10μM. **(C)** Quantification of ciliogenesis in MKs shifted to 2mM Ca^{+2} media and treated with increasing concentrations of chloral hydrate. Histogram represents mean data averaged from 2 independent experiments where ciliogenesis was quantified to determine the minimal effective concentration of chloral hydrate. Error bars are SEM.

Figure S5, related to Fig6. *Ift88* cKO epidermis displays defective ciliagenesis, reduced differentiation, and ectopic Notch signaling by E18.5 (A) Whole mount confocal microscopy of cilia from E17.5 vs E18.5 YFP (+) *Ift88* cKO epidermis. Arrows point to cilia visualized with an antibody against acetylated tubulin (red). Histogram represents quantification of ciliagenesis in YFP (+) cells in E17.5 vs E18.5 cKO epidermis, where 300-500 cells from 2-3 embryos were analyzed per condition. Note that cilia are not ablated until E18.5 in the *Ift88* cKO. Scale bars=10μM. Error bars are SEM. Note: K14-Cre *Ift88* cKO animals are mosaic, and survive postnatally. Analyses here are restricted to regions where IFT88 protein and cilia are missing**. (B)** *Ift88* cKO epidermis shows reduced levels of differentiation markers K10 and filaggrin in comparison to WT littermate controls. Scale bar=100μM. **(C)** *Ift88* cKO epidermis shows reduced but ectopic Notch signaling in comparison to WT controls. Note that Hes1 is ectopically expressed in K5 positive basal cells in *Ift88* cKO epidermis, but reduced in suprabasal cells in *Ift88* cKO epidermis. Scale bar=20μM. **(C')** Histograms show quantification of the % of Hes1 and NICD positive nuclei in

K5 positive (Basal) or K5 negative (Suprabasal) layers for mutant and WT cells, and are mean data averaged from 2-3 embryos. Error bars are SEM. Since Hes1 can be activated by Notch-independent pathways and is also not obligatory for the Notch-dependent basal to spinous cell switch, it is not possible to address whether this expression is due to alternative pathways, or merely the later stage ablation of Ift88 in the embryo. **Asymmetric cell division is normal in *Ift88* and *Kif3a* cKO epidermis. (D-E)** LGN is properly localized to an apical crescent in asymmetrically dividing *Ift88* and *Kif3a* cKO cells. YFP was used to confirm Cre activity in cKO tissue. Scale bars= 10μM.**(F)** Perpendicular and lateral spindle orientations are maintained in hypoproliferative *Kif3a* cKO epidermis. Histogram represents data from 3-4 different embryos, where only YFP(+) cells were analyzed. Data are represented as mean +/- SEM. Although cell proliferation is reduced in the *Kif3a* cKO epidermis, the relative numbers of lateral vs. perpendicular cell divisions, determined by spindle position in confocal WM images, are similar to WT. Representative confocal images are mitotic spindles in dividing basal cells in whole mount epidermis labeled with antibodies against pericentrin (red) and acetylated tubulin (green). Nuclei visualized with DAPI. Scale bar= 3μM

Figure S6, related to Fig6. Notch signaling is normal in *Shh* null developing epidermis, but ciliary mutants display abnormal hair follicle morphogenesis and defects in Shh signaling. (A) Immunolabeling in *Shh* KO sections of E17.5 backskins with Hes1, Notch3 receptor and the cleaved NICD3. Notch signaling components are equally expressed and properly localized in Shh null vs. WT littermate control tissue. * indicates background fluorescence**. (B)** Gli1 reporter activity (visualized with YFP) is only detected in developing HFs at E16.5, and is not detected in stratifying epidermis. Gli2 fluorescent *in situ* hybridization indicates that Gli2 in also only detected in developing HFs, not epidermis, at E16.5 **(C)** Abnormal HF morphogenesis is apparent by E18.5 in *Kif3a* cKO and *Ift74-1* transduced tissue in comparison to WT littermate or scrambled shRNA controls. **(D)** Gli2 is not detectable by *in situ* hybridization in stunted *Kif3a* cKO mutant HFs. **(E)** Gli2 levels are reduced in HFs transduced with *Ift74-1* lentivirus, in comparison to scrambled control infected hair follicles. **(F)** *Ift74-1* transduced embryos (RFP+) display polydactyly, which is never observed in non-infected littermate controls (RFP-, shown) or scrambled control embryos (not shown, see Beronja et al 2010). Note that in contrast to the skin epidermis (Croyle et al., 2011), limbs defective in ciliogenesis show loss of Gli3 repressor, leading to ectopic Shh signaling (Goetz and Anderson, 2010). A-D Scale bar=30μM, E Scale bar=10 μM.

Figure S7, related to Fig7. Notch3 and Presenilin-2 are expressed in suprabasal cells in developing epidermis. (A) Immunoblots of E17.5 epidermal lysates probed for Presenilin-2, Notch 3 receptor and enzymatically cleaved Notch3 Intracellular Domain (NICD3). **(B)** IF of saggittal sections of E17.5 epidermis stained with antibodies against Notch3 and Presenilin-2. Arrows point to bright puncta detected in suprabasal cells immunolabeled for Presenilin-2. Scale bar=30μM

Supplementary Experimental Procedures

Additional Mouse Strains Used

The generation of *K14-Cre* mice conditional for loss of function mutations in *β1 integrin* (Raghavan et al., 2000)*, α-catenin* (Vasioukhin et al., 2001)*, β-catenin* (Huelsken et al., 2001; Nguyen et al., 2009)*, FAK (Schober et al., 2007)* and *RBP-J* (Blanpain et al., 2006) and NICD-GFP (Blanpain et al., 2006), Gli1CreER as well as knockout mice for *Shh (Chiang et al., 1999)* and *p63* (Mills et al., 1999) have all been previously described. CD-1 mice obtained from Charles River Laboratories were used for *in utero* lentiviral injections as described previously (Beronja et al., 2010) but for *in vivo* rescue experiments injections were performed using K14-Cre NICD-GFP transgenic mice (Blanpain et al., 2006). For Gli1 induction, tamoxifen (Sigma) was dissolved in corn oil to a final concentration of 20mg/ml and pregnant Gli2CreER,R26YFP females received 0.5 ml of tamoxifen by oral gavage for 3 consecutive days.

ShRNA hairpin sequences

The shRNAs targeted the following sequences:

Ift80-1 5’CCTCAGACTTAGAGTCTAAAT3’
Ift80-2 5’CGGCAGTGATTAGTCTCTCAT3’
Ift172-1 5’GCGGCCATCAACCACTATATT3’
Ift172-2 5’GCTGCTGATCTCTCATTACTA3’
Ift52 5’GCTCATCTGGAACATGATATT3’
Ift57-1 5’GCATTATTGAAGAGTAGCTTT3’
Ift57-2 5’CGCAGCTGAAAGTCACGATTA3’
Ift74-1 5’GCCGACTGAGTCTACAAGCAT3’ (sequence in 3’ UTR)

Ift74-2 5'CCTCAGATTATGATACCCTTA3'
Ift88-1 5'GCCCTCAGATAGAAAGACCAA3'
Ift88-2 5'GCCAAATAAGTCATTTACCAA3' (sequence in 3' UTR)

Scrambled control sequence is
5'CAACAAGATGAAGAGCACCAA3'

For *in vitro* shRNA rescue experiments, non-targeted *Ift74* rat cDNA and *Ift88* mouse cDNA (AccessionNumbers: BC083611, BC012250) were obtained from Open Biosystems. Coding sequences from each cDNA were subcloned into the EcoRI and XhoI sites of the pCMV-HA vector from Clontech (Cat. No 631604) and *Ift* KD cell lines were transfected (Fugene) and analyzed for ciliagenesis and cell proliferation 24-48 hrs post-transfection.

Embryo preparation, *in vivo* immunofluorescence, and immunoblot analyses

Assays to determine skin barrier function have been described (Segre et al., 1999). 3hr prior to the desired stage of development, BrdU (50 µg/g) was injected intraperitonally in pregnant females and embryos were then processed. Typically, >3 embryos from independent experiments were analyzed for each condition.

For whole-mount immunofluorescence, embryos were fixed in 4% formaldehyde in PBS for 1 hour at room temperature and washed extensively in phosphate buffered saline (PBS). Backskins were dissected and then permeabilized for 10 minutes in 0.3% Triton/PBS and blocked in Gelatin Block (2.5% fish gelatin, 2.5% normal donkey serum, 2.5% normal goat serum, 0.5% BSA, 0.3% Triton, 1X PBS) containing MOM reagent (Vector Laboratories) for 1 hour at room temperature. All primary antibodies were used at 1:200 dilution and incubated overnight at 4°C. Primary antibodies were removed by extensive washing in 0.3% triton/PBS, followed by 1 hour RT incubation with secondary antibodies (see below).

For immunofluorescence on sagittal sections, embryos were embedded and frozen in OCT, cryosectioned (10–12um) and fixed 10 minutes in 4% formaldehyde in PBS. Sections

were blocked 1 hour in 2.5% fish gelatin, 2.5% normal donkey serum, 2.5% normal goat serum, 0.5% BSA, 0.1% Triton, 1X PBS. The following primary antibodies were incubated for either 2 hours at room temperature or overnight at 4°C at the following dilutions: mouse monoclonal anti-acetylated α-tubulin (Sigma, 1:300), mouse monoclonal E-cadherin (Fuchs lab, 1:200), rabbit anti–Ki67 (Covance, 1:500), rabbit anit-kinesin II (Sigma, 1:500), rat anti-α-tubulin (Millipore, 1:200), rabbit anti-Ift88 (ProteinTech, 1:200) rabbit anti–K14 (Fuchs lab, 1:400), rat anti-BrdU (Abcam, 1:200), rat anti–Nidogen (Invitrogen 1:2000), rabbit anti–K10 (Covance, 1:500), rabbit anti-involucrin (Covance, 1:1000), rabbit anti-filaggrin (Covance, 1:1000), rabbit anti-Hes1 (Fuchs lab, 1:1000), chicken anti-GFP (Abcam, 1:5000), rabbit anti-GFP (Invitrogen, 1:5000), hamster monoclonal anti-Notch3 (Biolegend, 1:400), rabbit anti-Notch3/NICD3 (Abcam ab23426, 1:400), rabbit anti–Presenilin-2 (Abcam, 1:200), rabbit anti-Gli2 (abcam) and rabbit anit-caspase3 (AF835, 1:1000 R&D). Secondary antibodies conjugated to Alexa-488 (Molecular Probes), FITC, Cy3, RRX, or Cy5 (Jackson Laboratories) were diluted 1:200-1:500 in gelatin block and incubated 1 hour at room temperature. Tissue was extensively washed in PBS prior to mounting with Pro-Long Gold containing DAPI (Invitrogen). In situ hybridization (ISH) for Gli2 was performed as previously described except that Tyramide-Signal Amplification (TSA) (Perkin-Elmer, Cy5 secondary) was used to enhance the Gli2 ISH signal, which was weakly detected in hair follicles in early embryonic tissue (E15.5-16.5). This step was added in order to determine if any Gli2 signal could also be detected in the epidermis.

Immunoblots

Cultured keratinocytes or dispase-treated and homogenized epidermal tissues were lysed in RIPA buffer containing a cocktail of protease inhibitors (Roche). Gel electrophoresis, Western blotting and infrared imaging using an Odessey scanner were performed using standard

methodology (Invitrogen). Primary antibodies used were goat anti-Ift74 (Sigma, 1:1000), goat anti-Ift88 (Sigma, 1:500), mouse anti-acetylated tubulin (Sigma, 1:1000), rabbit anti-E-cadherin (Fuchs lab, 1:1000), rat anti-αtubulin (Millipore, 1:5000), Hamster monoclonal anti-Notch3 (Biolegend, 1:500), rabbit anti-Notch3/NICD3 (Abcam ab23426, 1:500), rabbit anti-Presenilin-2 (Abcam, 1:100,000). Secondary antibodies were conjugated to IRDye680 or IRDye800CW (LiCor and Rockland) and were used at 1:15000.

Confocal microscopy and imaging

Confocal images were acquired with a Zeiss LSM510 laser-scanning microscope (Carl Zeiss MicroImaging) through a 63x oil objective. (N.A. 1.4) For whole mount imaging, Z-stacks of 20-40 planes (0.25μm) were captured, but only representative single Z-planes are presented, except in Figure 2G and Supplemental Figure2B a Z projection of the entire MT cytoskeleton is shown. Images were recorded at either 512x512 or 1024×1024 square pixels. For wide-field epifluorescence images were acquired using a Zeiss Axioplan 2 20x/0.8 air or 63x/1.4 oil Plan-Apochromat objectives and equipped with the following Chroma filter sets: 49003 ET YFP (YFP), 49008 ET TR C94094 (mRFP1), 49004 ET dsR C94093 (Cy3, DyLight549), 41008 Cy5 (Cy5), 41001 FITC (AlexaFluor 488/GFP). For analysis of MT dynamics, cultured keratinocytes stably expressing scrambled shRNA or Ift74-1 shRNAs were transiently transfected with mCherry-tubulin (Invitrogen) 24 hours prior to imaging. Time series were acquired on a Spinning Disk Confocal (Zeiss) equipped with a 100× α-plane Fluor (1.45 oil) lens and an EM charge coupled device camera (Hamamatsu). Cells expressing low levels of mCherry-tubulin were selected and images acquired every 5-10 seconds for 15-20 minutes in order to capture MT dynamics. Stacks were exported from Velocity software into Metamorph (Universal Imaging), where individual MTs were then manually tracked and the % of time spent in pause, growth or catastrophe was determined.

Quantification and statistical analysis

For quantification of ciliogenesis and Ki67 expression during epidermal development or in cultured keratinocytes, the number of nuclei were determined in single confocal planes by thresholding the image (either DAPI, Ki67(+) or H2B-RFP (+) nuclei) in ImageJ and using the Measure function to count the number of objects. The number of cilia were then manually counted in either basal or suprabasal single Z-planes from confocal stacks. Quantifications of BrdU and phospho-H3 levels were performed using similar methods. Kif3a and Ift88 cKOs were generated on a YFP Rosa 26 loxstoplox background, and only YFP (+) cells were quantified in all instances where cKO tissue was analyzed. For quantifications of E-cadherin, Notch3 and Presenilin-2 ciliary localization, the number of nuclei was determined using the measure function in ImageJ and then the number of cilia with co-localization of either protein was manually determined in merged images of confocal Z-stacks of basal and suprabasal cells. For quantification of Notch reporter activity, individual cells expressing H2B-RFP fluorescence were outlined and the average gray value of the GFP signal was determined using the measure function in ImageJ. For quantification of *Kif3a*/YFP(+)/NICD(-) mosaic analysis, cells were identified as "suprabasal" based on their lack of K14 and/or β1 integrin expression. For quantification of Hes1 and NICD positive *Ift88* cKO cells, nuclei in either K5 (+) basal or K5(-) suprabasal YFP(+) cells were thresholded in ImageJ, and the number of Hes1, NICD, and DAPI nuclei were counted. Unless otherwise noted, all error bars represent standard error of the mean (SEM) and where indicated an unpaired 2 tailed student's t-test was performed on data sets collected from multiple independent experiments in order to determine statistical significance.

Supplementary References

Jaulin, F., and Kreitzer, G. (2010). KIF17 stabilizes microtubules and contributes to epithelial morphogenesis by acting at MT plus ends with EB1 and APC. J Cell Biol *190*, 443-460.

Beronja, S., Livshits, G., Williams, S., and Fuchs, E. (2010). Rapid functional dissection of genetic fetworks via tissue specific transduction and RNAi in mouse embryos. Nature Medicine.

Blanpain, C., Lowry, W. E., Pasolli, H. A., and Fuchs, E. (2006). Canonical notch signaling functions as a commitment switch in the epidermal lineage. Genes Dev *20*, 3022-3035.

Chiang, Y., Rizzino, A., Sibenaller, Z. A., Wold, M. S., and Vishwanatha, J. K. (1999). Specific down-regulation of annexin II expression in human cells interferes with cell proliferation. Mol Cell Biochem *199*, 139-147.

Huelsken, J., Vogel, R., Erdmann, B., Cotsarelis, G., and Birchmeier, W. (2001). beta-Catenin controls hair follicle morphogenesis and stem cell differentiation in the skin. Cell *105*, 533-545.

Mills, A. A., Zheng, B., Wang, X. J., Vogel, H., Roop, D. R., and Bradley, A. (1999). p63 is a p53 homologue required for limb and epidermal morphogenesis. Nature *398*, 708-713.

Nguyen, H., Merrill, B., Polak, L., Nikolova, M., Rendl, M., Shaver, T., Pasoll, i. H., and Fuchs, E. (2009). Tcf3 and Tcf4 are essential for long-term homeostasis of skin epithelia. Nature Genetics.

Raghavan, S., Bauer, C., Mundschau, G., Li, Q., and Fuchs, E. (2000). Conditional ablation of beta1 integrin in skin. Severe defects in epidermal proliferation, basement membrane formation, and hair follicle invagination. J Cell Biol *150*, 1149-1160.

Schober, M., Raghavan, S., Nikolova, M., Polak, L., Pasolli, H. A., Beggs, H. E., Reichardt, L. F., and Fuchs, E. (2007). Focal adhesion kinase modulates tension signaling to control actin and focal adhesion dynamics. J Cell Biol *176*, 667-680.

Vasioukhin, V., Bauer, C., Degenstein, L., Wise, B., and Fuchs, E. (2001). Hyperproliferation and defects in epithelial polarity upon conditional ablation of alpha-catenin in skin. Cell *104*, 605-617.

Supplemental Figure1

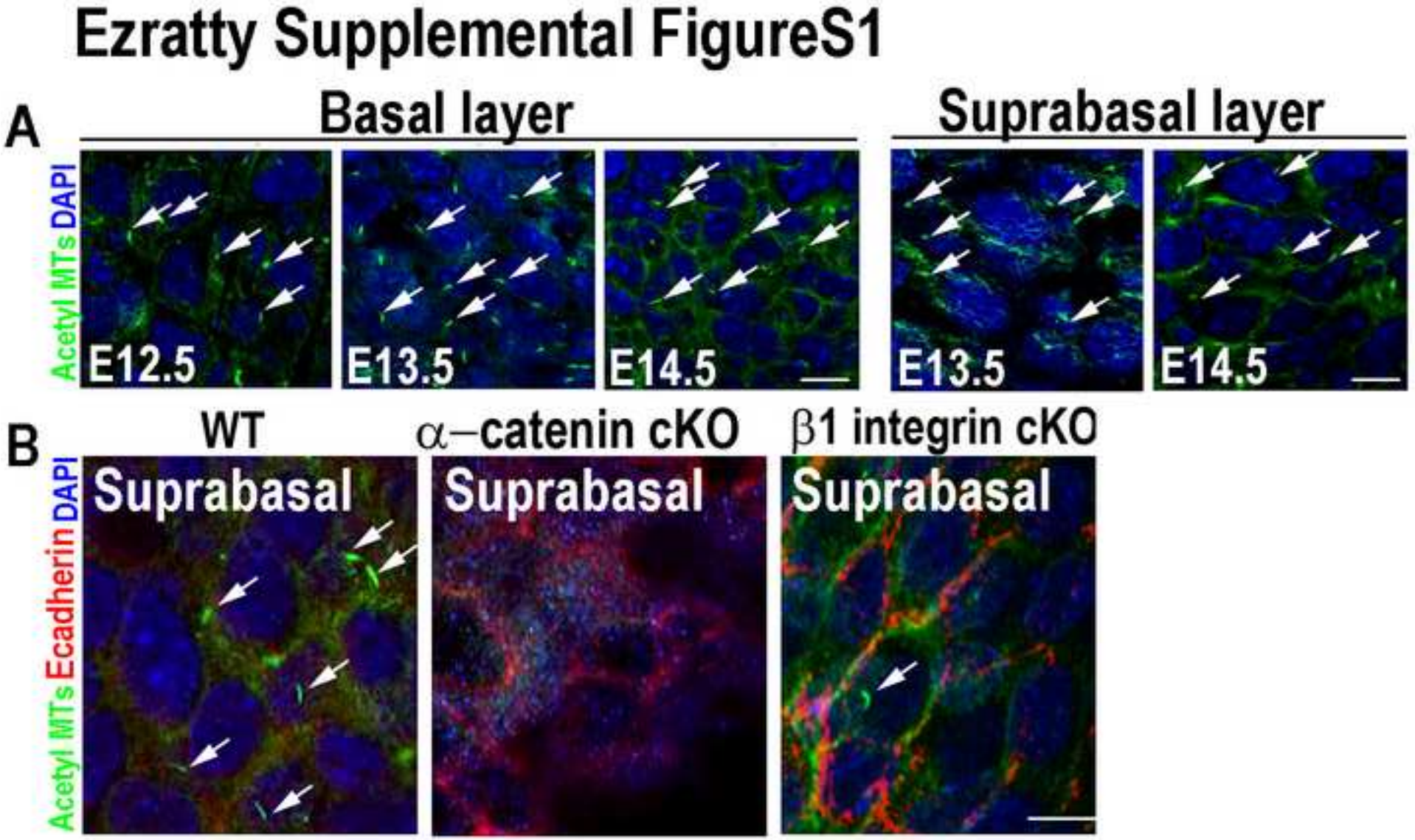

Supplemental Figure2

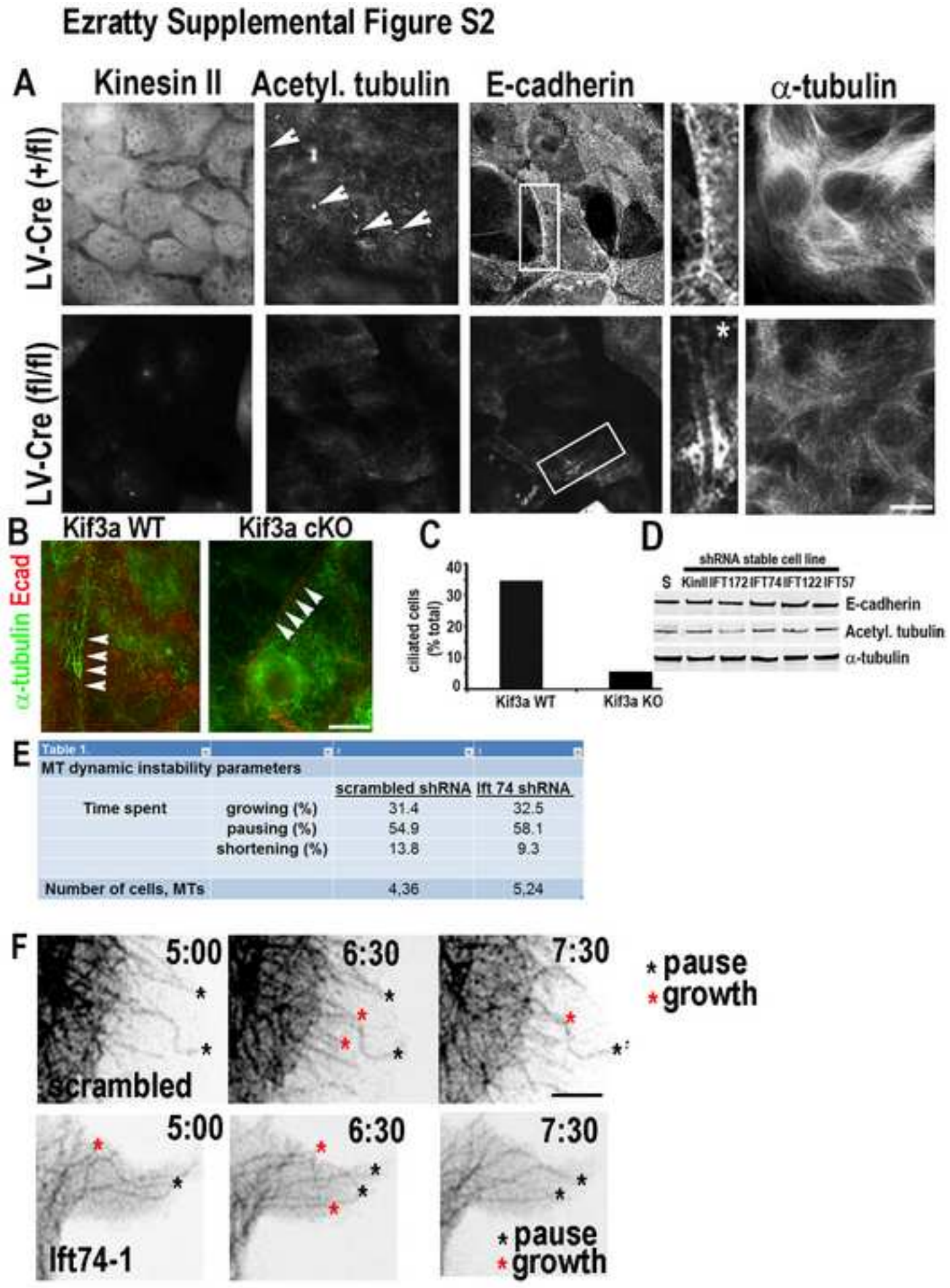

Ezratty Supplemental Figure S3

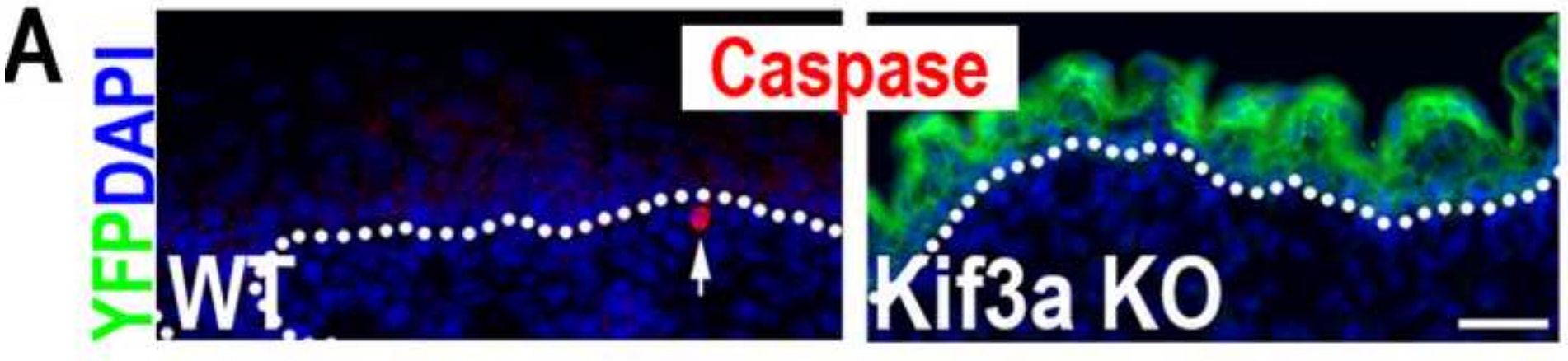

Supplemental Figure4

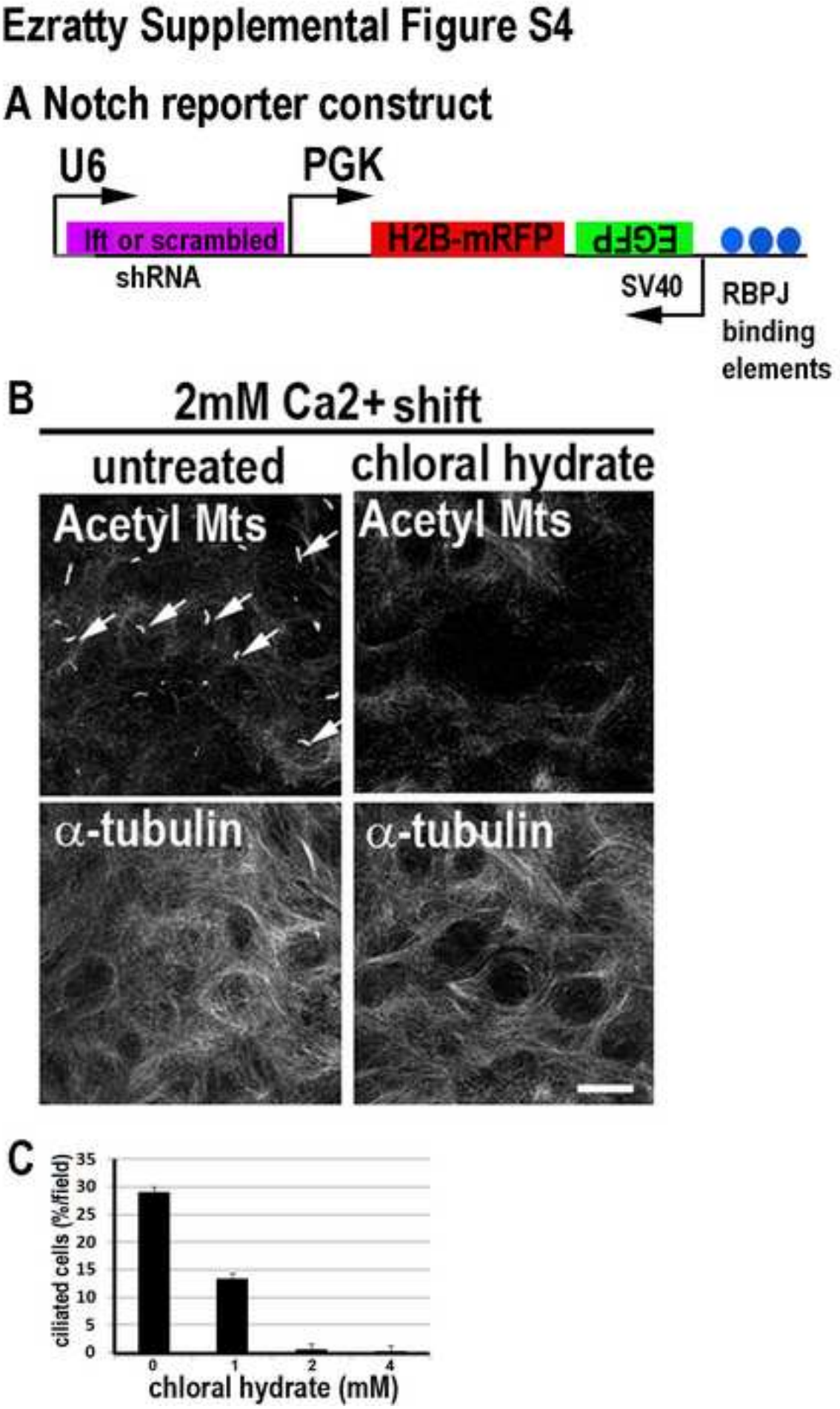

Supplemental Figure5

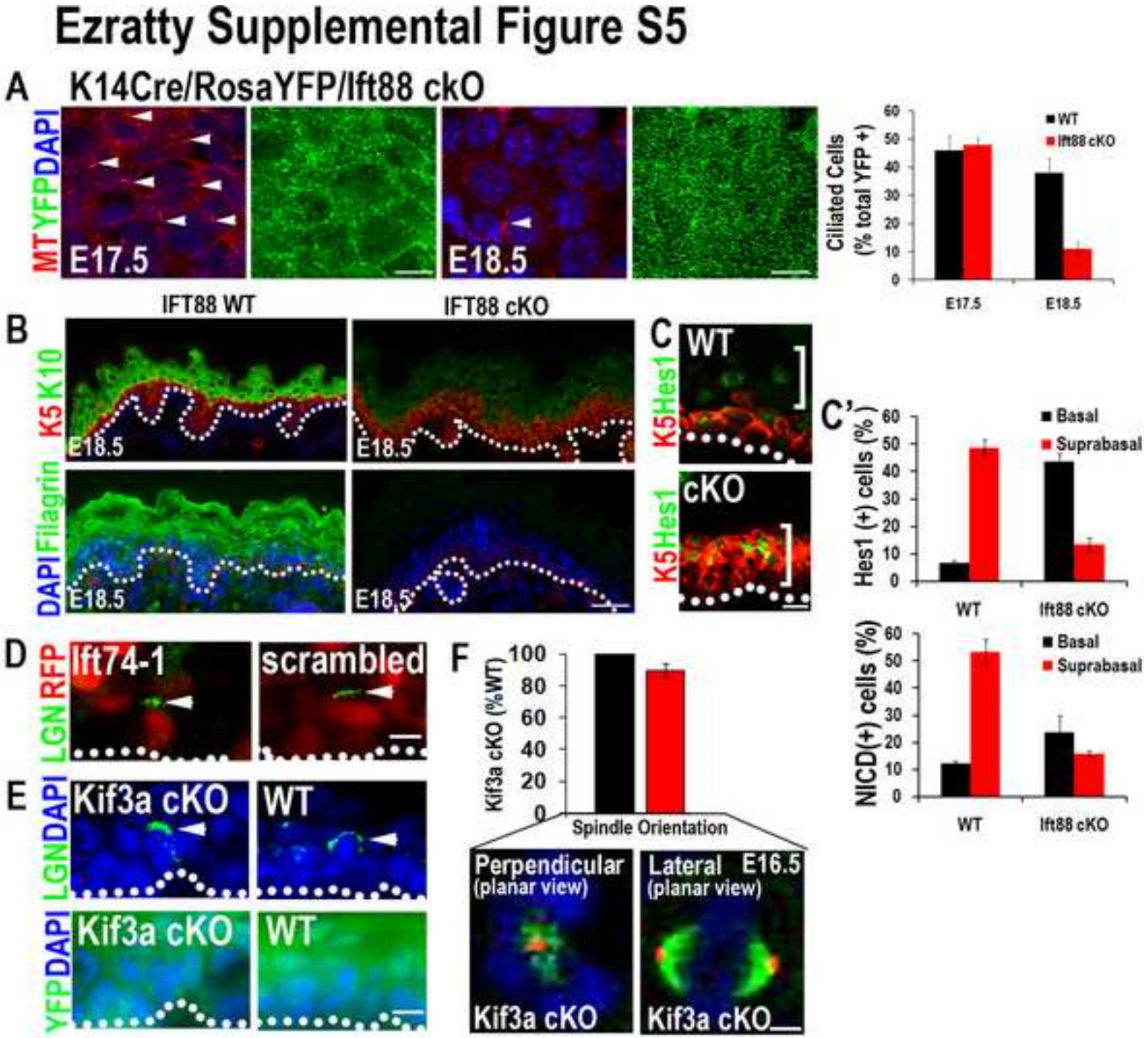

Supplemental Figure6

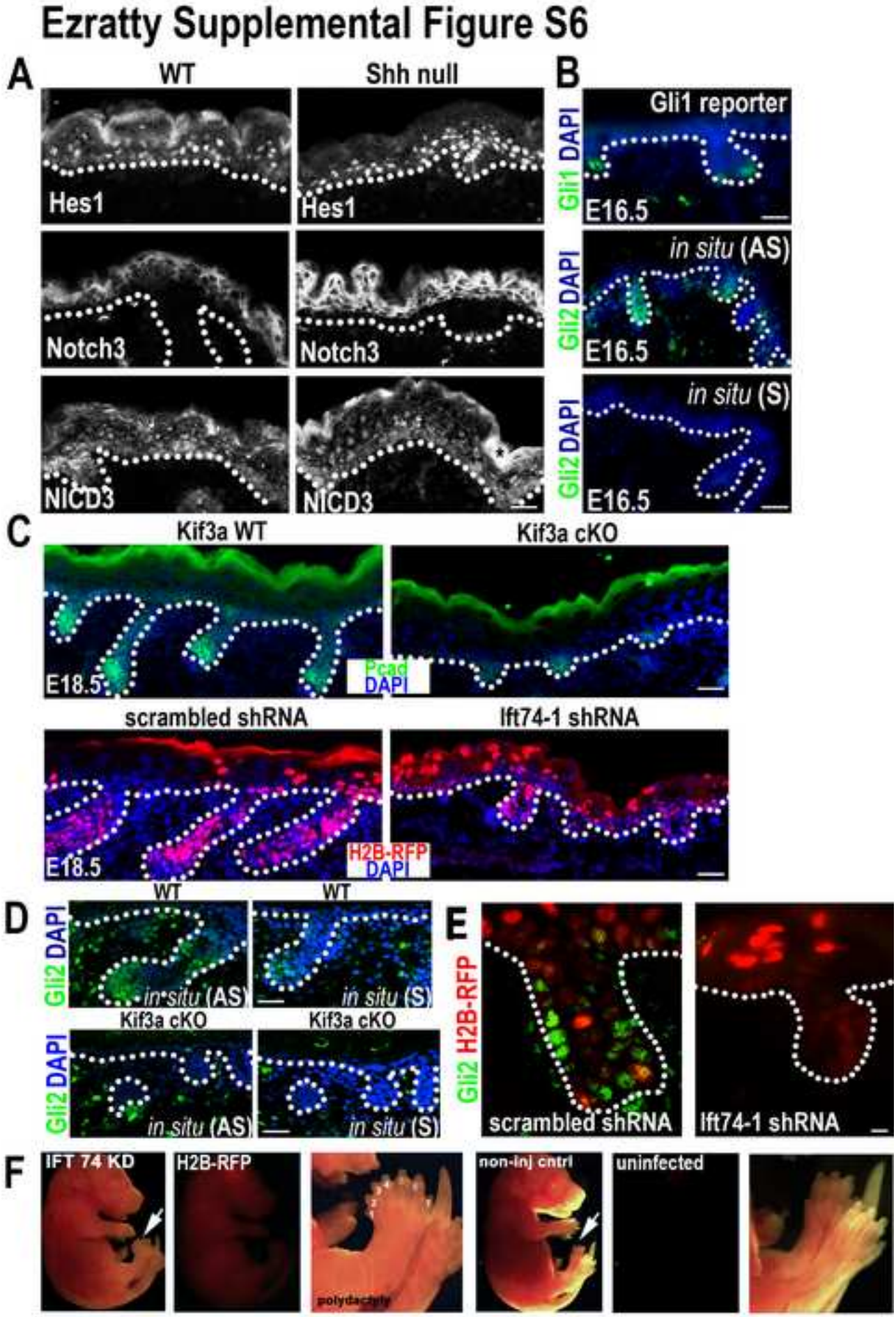

Supplemental Figure7